



## Multiple-relaxation-time lattice Boltzmann model-based four-level finite-difference scheme for one-dimensional diffusion equations

Yuxin Lin <sup>1</sup>, Ning Hong,<sup>2</sup> Baochang Shi,<sup>1,3</sup> and Zhenhua Chai <sup>1,3,\*</sup>

<sup>1</sup>*School of Mathematics and Statistics, Huazhong University of Science and Technology, Wuhan 430074, China*

<sup>2</sup>*School of General Education, Wuchang University of Technology, Wuhan 430223, China*

<sup>3</sup>*Hubei Key Laboratory of Engineering Modeling and Scientific Computing, Huazhong University of Science and Technology, Wuhan 430074, China*



(Received 20 December 2020; revised 23 April 2021; accepted 28 June 2021; published 26 July 2021)

In this paper, we first present a multiple-relaxation-time lattice Boltzmann (MRT-LB) model for one-dimensional diffusion equation where the D1Q3 (three discrete velocities in one-dimensional space) lattice structure is considered. Then through the theoretical analysis, we derive an explicit four-level finite-difference scheme from this MRT-LB model. The results show that the four-level finite-difference scheme is unconditionally stable, and through adjusting the weight coefficient  $\omega_0$  and the relaxation parameters  $s_1$  and  $s_2$  corresponding to the first and second moments, it can also have a sixth-order accuracy in space. Finally, we also test the four-level finite-difference scheme through some numerical simulations and find that the numerical results are consistent with our theoretical analysis.

DOI: [10.1103/PhysRevE.104.015312](https://doi.org/10.1103/PhysRevE.104.015312)

### I. INTRODUCTION

In the past decades, the lattice Boltzmann (LB) method, as one of the mesoscopic numerical approaches, not only has gained a great success in the study of complex flows governed by the Navier-Stokes equations [1–13] but also can be considered as a numerical solver to some other types of the partial differential equations, for example, the diffusion equations [14–18], convection-diffusion equations [19–30], Poisson equation [31–33], Kuramoto-Sivashinsky equations [34–36], and some complex equations [37–40]. Based on the collision term in the LB method, the LB models can be classified into three basic kinds, i.e., the lattice BGK or single-relaxation-time LB (SRT-LB) model [41], two-relaxation-time LB (TRT-LB) model [20], and the multiple-relaxation-time LB (MRT-LB) model [42]. Actually, the SRT-LB and TRT-LB models are two special cases of the MRT-LB model [43], and moreover, the MRT-LB model could be more stable and/or more accurate than SRT-LB and TRT-LB models through adjusting some free relaxation parameters [44–47]. For these reasons, the MRT-LB model is considered in this work.

To build the relation between the LB method and the macroscopic partial differential equations, some asymptotic analysis approaches are usually adopted [43], including the Chapman-Enskog expansion [48], Maxwell iteration [49,50], direct Taylor expansion [51–53], recurrence equation [54,55], and asymptotic expansion with diffusive scaling [56]. With the help of these asymptotic analysis methods, one can determine the expression of macroscopic transport efficient, which is related to the relaxation parameter appeared in the LB model.

Although the asymptotic analysis methods can be used to illustrate that the LB method is suitable for the macroscopic partial differential equations, and also the accuracy of the LB method [53,57,58], the relation between the mesoscopic LB method and the macroscopic partial-differential-equation based numerical schemes (hereafter named macroscopic numerical schemes) is still unclear, and furthermore, can we obtain the macroscopic numerical scheme of the LB method? Actually, once the macroscopic numerical scheme of the LB method is obtained, we can not only gain a better understanding on the LB method through the knowledge already available on the macroscopic numerical scheme, but also perform more further research on constructing the mesoscopic LB models for macroscopic partial differential equations.

In the past years, some efforts have been made on this aspect. Junk [59] and Inamuro [60] found that when the relaxation parameter is equal to unity, the SRT-LB model would reduce to a special macroscopic two-level finite-difference scheme, and at the diffusive scaling ( $\Delta t \propto \Delta x^2$ ,  $\Delta t$  and  $\Delta x$  are time step and lattice spacing), the macroscopic numerical scheme for the incompressible Navier-Stokes equations has a second-order convergence rate in space [59]. Ancona [61] demonstrated that for one-dimensional convection-diffusion equations, the LB method with D1Q2 lattice structure can be written as the classical DuFort-Frankel scheme [62], which is an explicit three-level second-order finite-difference scheme. He *et al.* [63] performed a theoretical analysis on the SRT-LB model for several simple flows, and found that when the flows are assumed to be unidirectional and steady-state, the SRT-LB mode is nothing but a macroscopic second-order finite-difference scheme of simplified incompressible Navier-Stokes equations. Then they also obtained the analytical solutions of these simple flows under some commonly used schemes for nonslip boundary conditions, and demonstrated

\*hustczh@hust.edu.cn

that usually there is a numerical slip velocity at the solid wall which cannot be eliminated effectively in the SRT-LB model. Following the same way, Guo and his collaborators [64,65] conducted some analyses on the MRT-LB model for microscale flows, and obtained the similar results as those reported in Ref. [63], while the numerical slip caused by the bounce-back scheme can be eliminated through adjusting the free relaxation parameter corresponding the third-order moment of the distribution function. d’Humière and Ginzburg [54] carried out a theoretical analysis on the TRT-LB model with recurrence equations, and found that when the relation  $\Lambda^{\text{eo}} = 1/4$  ( $\Lambda^{\text{eo}}$  is the so-called *magic* parameter) is satisfied, the TRT-LB model would become a macroscopic three-level finite-difference scheme with a second-order accuracy in space. Subsequently, Ginzburg [55] further performed a comprehensive analysis on the TRT-LB model, and found that under the conditions of  $\Lambda^{\text{eo}} = 1/6$  and  $\Lambda_{\text{BGK}} = 1/12$ , an “optimal diffusion” TRT-LB model with a fourth-order accuracy in space can be obtained. However, the “optimal diffusion” TRT-LB model based macroscopic finite-difference scheme for the diffusion equation is still unclear. Li *et al.* [66] conducted an analysis on the SRT-LB model with D1Q2 lattice structure for one-dimensional Burgers equation, and demonstrated that this LB model is equivalent to an explicit three-level second-order finite-difference scheme. Recently, Cui *et al.* [46] also carried out a theoretical analysis on the MRT-LB model for the convection-diffusion equation, and found that for the unidirectional and steady-state problems, the MRT-LB model is just a macroscopic second-order finite-difference scheme of convection-diffusion equation. From the works mentioned above, one can see that under some special conditions, the LB method is equivalent to a special macroscopic second-order finite-difference scheme for a specified partial differential equation, which is also consistent with the results of some asymptotic analyses on the LB method [43]. However, through choosing the weight coefficients and relaxation parameter properly, Suga [17] found that the SRT-LB model with D1Q3 lattice structure could be a macroscopic four-level fourth-order finite-difference scheme for one-dimensional diffusion equation. We noted that this work is only limited to the SRT-LB model, it is still unclear whether the more general MRT-LB model can be written as a macroscopic high-order finite-difference scheme, and additionally, can we obtain a more accurate finite-difference scheme from the MRT-LB model where more degrees of freedom in adjusting the relaxation parameters are included? To answer these questions, in this work we first develop a MRT-LB model for one-dimensional diffusion equation where a free weight coefficient  $\omega_0$  is introduced, and then based on this MRT-LB model, we obtain an equivalent macroscopic four-level finite-difference scheme. Through some theoretical analyses, we show that the four-level finite-difference scheme is unconditionally stable, and can achieve a sixth-order convergence rate in space through adjusting some free parameters.

The rest of the paper is organized as follows. In Sec. II, we presented a MRT-LB model for the one-dimensional diffusion equations where the D1Q3 lattice structure is adopted, and then derived an explicit four-level finite-difference scheme from the MRT LB model. Additionally, it is also shown that

the macroscopic numerical schemes of the SRT-LB model, TRT-LB model, regularized-LB model and modified-lattice-kinetic model are just some special cases of that of the MRT-LB model. In Sec. III, we investigated the accuracy of the four-level finite-difference scheme, followed by a stability analysis in Sec. IV. In Sec. V, we performed some simulations, and found that under some conditions, the four-level finite-difference scheme has a sixth-order convergence rate in space, which is also consistent with our theoretical analysis. Finally, some conclusions are given in Sec. VI.

## II. MULTIPLE-RELAXATION-TIME LATTICE BOLTZMANN MODEL BASED FOUR-LEVEL FINITE-DIFFERENCE SCHEME FOR ONE-DIMENSIONAL DIFFUSION EQUATION

In this section, we first developed a MRT-LB model for one-dimensional diffusion equation with a constant diffusion coefficient, and then presented the details on how to obtain an explicit four-level finite-difference scheme from the MRT-LB model.

### A. The MRT-LB model for one-dimensional diffusion equation

From the mathematical point of view, the one-dimensional diffusion process of mass and heat can be described by the classical diffusion equation,

$$\frac{\partial \phi}{\partial t} = \kappa \frac{\partial^2 \phi}{\partial x^2} + R, \quad (1)$$

where  $\phi$  is a scalar variable dependent on the space  $x$  and time  $t$ .  $\kappa$  is the diffusion coefficient,  $R$  is the source term, and in this work, they are assumed to be two constants. In the framework of LB method, the diffusion Eq. (1) can be solved efficiently and accurately [14,15,17,20,25,28], here we only consider the more general MRT-LB model for its accuracy and stability in the study of complex problems [45,47,67].

The evolution of MRT-LB model for the diffusion Eq. (1) can be written as [28,46]

$$\begin{aligned} f_i(x + \mathbf{c}_i \Delta t, t + \Delta t) &= f_i(x, t) - (\mathbf{M}^{-1} \mathbf{S} \mathbf{M})_{ik} [f_k(x, t) - f_k^{\text{eq}}(x, t)] \\ &+ \Delta t \left[ \mathbf{M}^{-1} \left( \mathbf{I} - \frac{\mathbf{S}}{2} \right) \mathbf{M} \right]_{ik} R_k, \quad (i = -1, 0, 1), \end{aligned} \quad (2)$$

where  $f_i(x, t)$  and  $f_i^{\text{eq}}(x, t)$  are the distribution function and equilibrium distribution at position  $x$  and time  $t$ . In the D1Q3 lattice structure, the discrete velocity  $\mathbf{c}_i$ , the transformation matrix  $\mathbf{M}$ , and the diagonal relaxation matrix  $\mathbf{S}$  can be given by

$$\mathbf{c}_i = \begin{cases} -c, & i = -1, \\ 0, & i = 0, \\ c, & i = 1, \end{cases} \quad (3a)$$

$$\mathbf{M} = \begin{pmatrix} 1 & 1 & 1 \\ -c & 0 & c \\ c^2 & -2c^2 & c^2 \end{pmatrix}, \quad (3b)$$

$$\mathbf{S} = \begin{pmatrix} s_0 & 0 & 0 \\ 0 & s_1 & 0 \\ 0 & 0 & s_2 \end{pmatrix}, \quad (3c)$$

where  $c = \Delta x / \Delta t$  is the lattice speed with  $\Delta x$  and  $\Delta t$  being lattice spacing and time step, respectively. The diagonal element  $s_i$  of the relaxation matrix  $\mathbf{S}$  is the relaxation parameter corresponding to  $i$ th moment of the distribution function  $f_i(x, t)$ , and to make the physical transport coefficient (e.g., diffusion coefficient) positive, it should be located in the range  $(0, 2)$ .  $R_i$  is the discrete source term, and is defined by

$$R_i = \omega_i R, \quad (4)$$

where  $\omega_i$  is the weight coefficient.

In the LB method, to derive correct macroscopic diffusion Eq. (1), the equilibrium distribution should be defined as

$$f_i^{eq}(x, t) = \omega_i \phi(x, t), \quad (5)$$

which satisfies the following conditions [28],

$$\sum_i f_i^{eq}(x, t) = \phi(x, t), \quad (6a)$$

$$\sum_i \mathbf{c}_i f_i^{eq}(x, t) = 0, \quad (6b)$$

$$\sum_i \mathbf{c}_i \mathbf{c}_i f_i^{eq}(x, t) = 2\omega_1 \phi(x, t) c^2, \quad (6c)$$

where the relation  $\omega_{-1} = \omega_1$  derived from Eq. (6b) is used to obtain Eq. (6c). If the weight coefficient  $\omega_0$  is considered as a free parameter, then from Eq. (6a) and the condition  $\omega_{-1} = \omega_1$ , one can obtain

$$\omega_1 = \omega_{-1} = \frac{1 - \omega_0}{2}, \quad (7)$$

where  $0 < \omega_0 < 1$  which can be used to ensure that all weight coefficients are larger than zero. In addition, the macroscopic variable  $\phi(x, t)$  can be calculated by

$$\phi(x, t) = \sum_i f_i(x, t) + \frac{\Delta t}{2} R. \quad (8)$$

Through the Chapman-Enskog analysis [28], one can correctly recover the diffusion Eq. (1) from the present MRT-LB model with the following relation between the diffusion coefficient and relaxation parameter  $s_1$ ,

$$\kappa = 2\omega_1 \left( \frac{1}{s_1} - \frac{1}{2} \right) \frac{\Delta x^2}{\Delta t}. \quad (9)$$

### B. The MRT-LB model based explicit four-level finite-difference scheme

In this part, we will show some details on how to derive the macroscopic numerical scheme from the present MRT-LB model. To simplify the following analysis, the notations  $f_{i,j}^n = f_i(j\Delta x, n\Delta t)$  and  $\phi_j^n = \phi(j\Delta x, n\Delta t)$  are introduced. Through substituting the discrete source term  $R_i$  [Eq. (4)] and equilibrium distribution function [Eq. (5)] into the evolution Eq. (2), we have

$$f_{-1,j}^{n+1} = f_{-1,j+1}^n - \frac{s_1}{2} (f_{-1,j+1}^n - f_{1,j+1}^n) + \frac{s_2}{2} f_{0,j+1}^n - \frac{\omega_0 s_2}{2} \phi_{j+1}^n + \left( \omega_{-1} + \frac{\omega_0 s_2}{4} \right) \Delta t R, \quad (10a)$$

$$f_{0,j}^{n+1} = f_{0,j}^n - s_2 f_{0,j}^n + \omega_0 s_2 \phi_j^n + \omega_0 \left( 1 - \frac{s_2}{2} \right) \Delta t R, \quad (10b)$$

$$f_{1,j}^{n+1} = f_{1,j-1}^n + \frac{s_1}{2} (f_{-1,j-1}^n - f_{1,j-1}^n) + \frac{s_2}{2} f_{0,j-1}^n - \frac{\omega_0 s_2}{2} \phi_{j-1}^n + \left( \omega_1 + \frac{\omega_0 s_2}{4} \right) \Delta t R, \quad (10c)$$

where Eq. (8) has been used. To obtain the macroscopic numerical scheme of the MRT-LB model, the distribution functions appeared in Eq. (10) must be replaced by the macroscopic variable  $\phi$  at different grid points and time levels. For this purpose, we first conduct a sum of Eq. (10), and derive the following equation:

$$\begin{aligned} \phi_j^{n+1} &= f_{-1,j+1}^n + f_{0,j}^n + f_{1,j-1}^n - \frac{s_1}{2} [(f_{-1,j+1}^n - f_{1,j+1}^n) - (f_{-1,j-1}^n - f_{1,j-1}^n)] \\ &\quad + \frac{s_2}{2} (f_{0,j-1}^n - 2f_{0,j}^n + f_{0,j+1}^n) - \frac{\omega_0 s_2}{2} (\phi_{j+1}^n - 2\phi_j^n + \phi_{j-1}^n) + \frac{3}{2} \Delta t R. \end{aligned} \quad (11)$$

Then from Eq. (10b) we can obtain

$$-f_{0,j}^n + s_2 f_{0,j}^n - \omega_0 s_2 \phi_j^n = -f_{0,j}^{n+1} + \omega_0 \left( 1 - \frac{s_2}{2} \right) \Delta t R. \quad (12)$$

Based on Eqs. (8), (10a), (10c), and (12), we have

$$f_{1,j+1}^n + f_{-1,j-1}^n = -f_{0,j}^n + \phi_j^{n-1} + \frac{1}{2} \Delta t R. \quad (13)$$

In addition, from Eq. (8) one can derive

$$\begin{aligned} f_{-1,j+1}^n + f_{0,j}^n + f_{1,j-1}^n &= -f_{-1,j-1}^n - f_{1,j+1}^n - f_{0,j-1}^n - f_{0,j+1}^n + f_{0,j}^n + \phi_{j+1}^n + \phi_{j-1}^n - \Delta t R \\ &= -(f_{0,j-1}^n - 2f_{0,j}^n + f_{0,j+1}^n) + \phi_{j+1}^n + \phi_{j-1}^n - \phi_j^{n-1} - \frac{3}{2} \Delta t R, \end{aligned} \quad (14)$$

where Eq. (13) has been adopted. Similarly, from Eqs. (8) and (13) we can also obtain

$$\begin{aligned} & (f_{-1,j+1}^n - f_{1,j+1}^n) - (f_{-1,j-1}^n - f_{1,j-1}^n) \\ &= -2(f_{1,j+1}^n + f_{-1,j-1}^n) - f_{0,j+1}^n - f_{0,j-1}^n + \phi_{j+1}^n + \phi_{j-1}^n - \Delta t R \\ &= -(f_{0,j-1}^n - 2f_{0,j}^n + f_{0,j+1}^n) + \phi_{j+1}^n + \phi_{j-1}^n - 2\phi_j^{n-1} - 2\Delta t R. \end{aligned} \tag{15}$$

Substituting Eqs. (14) and (15) into Eq. (11) yields

$$\begin{aligned} \phi_j^{n+1} &= \left(\frac{s_1}{2} + \frac{s_2}{2} - 1\right) \left(f_{0,j-1}^n - 2f_{0,j}^n + f_{0,j+1}^n\right) + \left(1 - \frac{s_1}{2} - \frac{\omega_0 s_2}{2}\right) \phi_{j+1}^n \\ &+ \omega_0 s_2 \phi_j^n + \left(1 - \frac{s_1}{2} - \frac{\omega_0 s_2}{2}\right) \phi_{j-1}^n + (s_1 - 1) \phi_j^{n-1} + \Delta t s_1 R. \end{aligned} \tag{16}$$

Now we need to give an evaluation of the first term on the right-hand side of Eq. (16). Actually, from Eqs. (8) and (10) we have

$$\begin{aligned} f_{0,j-1}^n - 2f_{0,j}^n + f_{0,j+1}^n &= f_{0,j-1}^n + f_{0,j+1}^n - 2(\phi_j^n - f_{-1,j}^n - f_{1,j}^n) + \Delta t R \\ &= 2(f_{-1,j}^n + f_{1,j}^n) + f_{0,j-1}^n + f_{0,j+1}^n - 2\phi_j^n + \Delta t R \\ &= f_{0,j+1}^{n-1} + 2f_{-1,j+1}^{n-1} + f_{0,j-1}^{n-1} + 2f_{1,j-1}^{n-1} \\ &- s_1[(f_{-1,j+1}^{n-1} - f_{1,j+1}^{n-1}) - (f_{-1,j-1}^{n-1} - f_{1,j-1}^{n-1})] - 2\phi_j^n + 3\Delta t R. \end{aligned} \tag{17}$$

With the help of Eqs. (8) and (13), one can derive the following equation,

$$\begin{aligned} & f_{0,j+1}^{n-1} + 2f_{-1,j+1}^{n-1} + f_{0,j-1}^{n-1} + 2f_{1,j-1}^{n-1} \\ &= -f_{0,j+1}^{n-1} - f_{0,j-1}^{n-1} - 2(f_{-1,j}^{n-1} + f_{1,j}^{n-1}) + 2\phi_{j+1}^{n-1} + 2\phi_{j-1}^{n-1} - 2\Delta t R \\ &= -(f_{0,j-1}^{n-1} - 2f_{0,j}^{n-1} + f_{0,j+1}^{n-1}) + 2\phi_{j+1}^{n-1} + 2\phi_{j-1}^{n-1} - 2\phi_j^{n-2} - 3\Delta t R. \end{aligned} \tag{18}$$

Substituting Eqs. (15) and (18) into Eq. (17) gives rise to

$$\begin{aligned} f_{0,j-1}^n - 2f_{0,j}^n + f_{0,j+1}^n &= (s_1 - 1)(f_{0,j-1}^{n-1} - 2f_{0,j}^{n-1} + f_{0,j+1}^{n-1}) \\ &- 2\phi_j^n + (2 - s_1)\phi_{j-1}^{n-1} + (2 - s_1)\phi_j^{n-2} - (2s_1 - 2)\phi_j^{n-2} + 2s_1 \Delta t R. \end{aligned} \tag{19}$$

If we substitute Eq. (19) into Eq. (16), then one can obtain

$$\begin{aligned} \phi_j^{n+1} &= (s_1 - 1) \left(\frac{s_1}{2} + \frac{s_2}{2} - 1\right) (f_{0,j-1}^{n-1} - 2f_{0,j}^{n-1} + f_{0,j+1}^{n-1}) \\ &+ \left(1 - \frac{s_1}{2} - \frac{\omega_0 s_2}{2}\right) \phi_{j-1}^n + \left[\omega_0 s_2 - 2\left(\frac{s_1}{2} + \frac{s_2}{2} - 1\right)\right] \phi_j^n \\ &+ \left(1 - \frac{s_1}{2} - \frac{\omega_0 s_2}{2}\right) \phi_{j+1}^n + (2 - s_1) \left(\frac{s_1}{2} + \frac{s_2}{2} - 1\right) \phi_{j-1}^{n-1} + (s_1 - 1) \phi_j^{n-1} \\ &+ (2 - s_1) \left(\frac{s_1}{2} + \frac{s_2}{2} - 1\right) \phi_{j+1}^{n-1} + (2s_1 - 2) \left(\frac{s_1}{2} + \frac{s_2}{2} - 1\right) \phi_j^{n-2} \\ &+ s_1(s_1 + s_2 - 1) \Delta t R. \end{aligned} \tag{20}$$

With the aid of Eq. (16), we can rewrite Eq. (20) as

$$\begin{aligned} \phi_j^{n+1} &= \left(1 - \frac{s_1}{2} - \frac{\omega_0 s_2}{2}\right) \phi_{j-1}^n + [(\omega_0 - 1)s_2 + 1] \phi_j^n + \left(1 - \frac{s_1}{2} - \frac{\omega_0 s_2}{2}\right) \phi_{j+1}^n \\ &+ \left(\frac{\omega_0 s_1 s_2}{2} - \frac{s_1 s_2}{2} - \frac{\omega_0 s_2}{2} + \frac{s_1}{2} + s_2 - 1\right) \phi_{j-1}^{n-1} + (-\omega_0 s_1 s_2 + \omega_0 s_2 + s_1 - 1) \phi_j^{n-1} \\ &+ \left(\frac{\omega_0 s_1 s_2}{2} - \frac{s_1 s_2}{2} - \frac{\omega_0 s_2}{2} + \frac{s_1}{2} + s_2 - 1\right) \phi_{j+1}^{n-1} + (s_1 - 1)(s_2 - 1) \phi_j^{n-2} + s_1 s_2 \Delta t R, \end{aligned} \tag{21}$$

which can also be written as

$$\phi_j^{n+1} = \alpha_1 \phi_{j-1}^n + \alpha_2 \phi_j^n + \alpha_1 \phi_{j+1}^n + \beta_1 \phi_{j-1}^{n-1} + \beta_2 \phi_j^{n-1} + \beta_1 \phi_{j+1}^{n-1} + \gamma \phi_j^{n-2} + \delta \Delta t R, \tag{22}$$

where the parameters  $\alpha_i$  ( $i = 1, 2$ ),  $\beta_i$ ,  $\gamma$ , and  $\delta$  are given by

$$\begin{aligned} \alpha_1 &= 1 - \frac{s_1}{2} - \frac{\omega_0 s_2}{2}, & \alpha_2 &= (\omega_0 - 1)s_2 + 1, \\ \beta_1 &= \frac{\omega_0 s_1 s_2}{2} - \frac{s_1 s_2}{2} - \frac{\omega_0 s_2}{2} + \frac{s_1}{2} + s_2 - 1, & \beta_2 &= -\omega_0 s_1 s_2 + \omega_0 s_2 + s_1 - 1, \\ \gamma &= (s_1 - 1)(s_2 - 1), & \delta &= s_1 s_2. \end{aligned} \tag{23}$$

Here we point out that Eq. (22) is the mesoscopic MRT-LB model based macroscopic explicit four-level finite-difference scheme for one-dimensional diffusion equation.

*Remark I:* If  $s_0 = s_1 = s_2 = \omega$  ( $\omega$  is the relaxation parameter in the SRT-LB model) and  $R = 0$ , then we can obtain the following SRT-LB model based four-level finite-difference scheme from Eq. (22),

$$\phi_j^{n+1} = \alpha_1 \phi_{j-1}^n + \alpha_2 \phi_j^n + \alpha_1 \phi_{j+1}^n + \beta_1 \phi_{j-1}^{n-1} + \beta_2 \phi_j^{n-1} + \beta_1 \phi_{j+1}^{n-1} + \gamma \phi_j^{n-2}, \tag{24}$$

with the following parameters:

$$\begin{aligned} \alpha_1 &= \Omega + \omega_1 \omega, & \alpha_2 &= \Omega + (1 - 2\omega_1)\omega, \\ \beta_1 &= -[\Omega + (1 - \omega_1)\omega]\Omega, & \beta_2 &= -(\Omega + 2\omega_1\omega)\Omega, & \gamma &= \Omega^2, \end{aligned} \tag{25}$$

where  $\Omega = 1 - \omega$ . It is clear that the SRT-LB model based macroscopic numerical scheme Eq. (24), as a special case of the present MRT-LB model based four-level scheme, is the same as that reported in the previous work [17].

*Remark II:* If  $s_0 = s_2 = s^+$  and  $s_1 = s^-$  with  $s^+$  and  $s^-$  denoting the relaxation parameters corresponding to the symmetric and antisymmetric modes [20], then we can obtain the TRT-LB model based four-level finite-difference scheme from Eq. (22). However, when  $s_0 = s_2 = 1$  and  $s_1 = \omega$ , one can derive the regularized-LB model [68,69] based macroscopic numerical scheme from Eq. (22). In addition, if  $s_0 = s_2 = \omega$

and  $s_1 = \omega/(1 - \omega\eta)$  with  $\eta$  being an adjusting parameter, we can also obtain the modified-lattice-kinetic model [70–72] based macroscopic numerical scheme from Eq. (22).

### III. THE ACCURACY ANALYSIS OF THE MRT-LB MODEL BASED MACROSCOPIC NUMERICAL SCHEME

We now performed an accuracy analysis on the macroscopic four-level finite-difference scheme Eq. (22). To do this, we first conducted the Taylor expansion to Eq. (22) at the position  $x = j\Delta x$  and time  $t = n\Delta t$ , and after some algebraic manipulations, one can obtain

$$\begin{aligned} (1 + 2\beta_1 + \beta_2 + 2\gamma) \left[ \frac{\partial \phi}{\partial t} \right]_j^n &= (\alpha_1 + \beta_1) \frac{\Delta x^2}{\Delta t} \left[ \frac{\partial^2 \phi}{\partial x^2} \right]_j^n + \delta R \\ &+ \frac{1}{12} (\alpha_1 + \beta_1) \frac{\Delta x^4}{\Delta t} \left[ \frac{\partial^4 \phi}{\partial x^4} \right]_j^n + \frac{1}{360} (\alpha_1 + \beta_1) \frac{\Delta x^6}{\Delta t} \left[ \frac{\partial^6 \phi}{\partial x^6} \right]_j^n \\ &- \beta_1 \Delta x^2 \left[ \frac{\partial^3 \phi}{\partial x^2 \partial t} \right]_j^n - \frac{\beta_1}{12} \Delta x^4 \left[ \frac{\partial^5 \phi}{\partial x^4 \partial t} \right]_j^n + \frac{\beta_1}{2} \Delta x^2 \Delta t \left[ \frac{\partial^4 \phi}{\partial x^2 \partial t^2} \right]_j^n \\ &+ \frac{1}{2} (2\beta_1 + \beta_2 + 4\gamma - 1) \Delta t \left[ \frac{\partial^2 \phi}{\partial t^2} \right]_j^n - \frac{1}{6} (2\beta_1 + \beta_2 + 8\gamma + 1) \Delta t^2 \left[ \frac{\partial^3 \phi}{\partial t^3} \right]_j^n + \dots \end{aligned} \tag{26}$$

Substituting Eq. (23) into above equation yields

$$\begin{aligned} \left[ \frac{\partial \phi}{\partial t} \right]_j^n &= \kappa \left[ \frac{\partial^2 \phi}{\partial x^2} \right]_j^n + R + \frac{1}{12} \kappa \Delta x^2 \left[ \frac{\partial^4 \phi}{\partial x^4} \right]_j^n + \frac{1}{360} \kappa \Delta x^4 \left[ \frac{\partial^6 \phi}{\partial x^6} \right]_j^n \\ &- \left( \frac{\omega_0}{2} - \frac{1}{2} - \frac{\omega_0}{2s_1} + \frac{1}{2s_2} + \frac{1}{s_1} - \frac{1}{s_1 s_2} \right) \Delta x^2 \left[ \frac{\partial^3 \phi}{\partial x^2 \partial t} \right]_j^n \\ &- \left( \frac{\omega_0}{24} - \frac{1}{24} - \frac{\omega_0}{24s_1} + \frac{1}{24s_2} + \frac{1}{12s_1} - \frac{1}{12s_1 s_2} \right) \Delta x^4 \left[ \frac{\partial^5 \phi}{\partial x^4 \partial t} \right]_j^n \\ &+ \left( \frac{\omega_0}{4} - \frac{1}{4} - \frac{\omega_0}{4s_1} + \frac{1}{4s_2} + \frac{1}{2s_1} - \frac{1}{2s_1 s_2} \right) \Delta x^2 \Delta t \left[ \frac{\partial^4 \phi}{\partial x^2 \partial t^2} \right]_j^n \\ &+ \left( \frac{3}{2} - \frac{1}{s_1} - \frac{1}{s_2} \right) \Delta t \left[ \frac{\partial^2 \phi}{\partial t^2} \right]_j^n + \left( \frac{1}{s_2} + \frac{1}{s_1} - \frac{7}{6} - \frac{1}{s_1 s_2} \right) \Delta t^2 \left[ \frac{\partial^3 \phi}{\partial t^3} \right]_j^n + \dots, \end{aligned} \tag{27}$$

where Eq. (9) has been used to derive above equation.

According to the diffusion Eq. (1), we have the following relations:

$$\begin{aligned} \left[ \frac{\partial^2 \phi}{\partial t^2} \right]_j^n &= \kappa^2 \left[ \frac{\partial^4 \phi}{\partial x^4} \right]_j^n, & \left[ \frac{\partial^3 \phi}{\partial t^3} \right]_j^n &= \kappa^3 \left[ \frac{\partial^6 \phi}{\partial x^6} \right]_j^n, \\ \left[ \frac{\partial^5 \phi}{\partial x^4 \partial t} \right]_j^n &= \kappa \left[ \frac{\partial^6 \phi}{\partial x^6} \right]_j^n, & \left[ \frac{\partial^3 \phi}{\partial x^2 \partial t} \right]_j^n &= \kappa \left[ \frac{\partial^4 \phi}{\partial x^4} \right]_j^n, & \left[ \frac{\partial^4 \phi}{\partial x^2 \partial t^2} \right]_j^n &= \kappa^2 \left[ \frac{\partial^6 \phi}{\partial x^6} \right]_j^n, \end{aligned} \tag{28}$$

Substituting Eq. (28) into Eq. (27), we have

$$\begin{aligned} \left[ \frac{\partial \phi}{\partial t} \right]_j^n &= \kappa \left[ \frac{\partial^2 \phi}{\partial x^2} \right]_j^n + R \\ &+ \frac{1}{s_1 s_2} \left[ \frac{s_1 s_2}{12} - \left( \frac{\omega_0 s_1 s_2}{2} - \frac{s_1 s_2}{2} - \frac{\omega_0 s_2}{2} + \frac{s_1}{2} + s_2 - 1 \right) + \left( \frac{3 s_1 s_2}{2} - s_2 - s_1 \right) \epsilon \right] \kappa \Delta x^2 \left[ \frac{\partial^4 \phi}{\partial x^4} \right]_j^n \\ &+ \frac{1}{s_1 s_2} \left[ \frac{s_1 s_2}{360} - \left( \frac{\omega_0 s_1 s_2}{24} - \frac{s_1 s_2}{24} - \frac{\omega_0 s_2}{24} + \frac{s_1}{24} + \frac{s_2}{12} - \frac{1}{12} \right) \right. \\ &+ \left. \left( \frac{\omega_0 s_1 s_2}{4} - \frac{s_1 s_2}{4} - \frac{\omega_0 s_2}{4} + \frac{s_1}{4} + \frac{s_2}{2} - \frac{1}{2} \right) \epsilon \right. \\ &+ \left. \left( -\frac{7 s_1 s_2}{6} + s_2 + s_1 - 1 \right) \epsilon^2 \right] \kappa \Delta x^4 \left[ \frac{\partial^6 \phi}{\partial x^6} \right]_j^n + O(\Delta x^6 + \Delta t^3), \end{aligned} \tag{29}$$

where  $\epsilon$  is the discretization parameter, and is defined by

$$\epsilon = \frac{\kappa \Delta t}{\Delta x^2} = 2\omega_1 \left( \frac{1}{s_1} - \frac{1}{2} \right) = (1 - \omega_0) \left( \frac{1}{s_1} - \frac{1}{2} \right). \tag{30}$$

From above discussion, it is clear that for a given diffusion coefficient  $\kappa$  (or discretization parameter  $\epsilon$ ), one can obtain an explicit four-level finite-difference scheme with the third-order accuracy in time and sixth-order accuracy in space once the following conditions are satisfied, i.e., the second and fourth-order truncation errors in Eq. (29) are equal to zero,

$$\frac{s_1 s_2}{12} - \left( \frac{\omega_0 s_2}{2} + \frac{s_1}{2} - 1 \right) + \left( \frac{s_1 s_2}{2} - s_2 - s_1 \right) \epsilon = 0, \tag{31a}$$

$$\frac{s_1 s_2}{360} - \frac{1}{12} \left( \frac{\omega_0 s_2}{2} + \frac{s_1}{2} - 1 \right) - \frac{1}{2} \left( \frac{s_1 s_2}{6} - \frac{\omega_0 s_2}{2} - \frac{s_1}{2} + 1 \right) \epsilon + \left( -\frac{2 s_1 s_2}{3} + s_2 + s_1 - 1 \right) \epsilon^2 = 0, \tag{31b}$$

where Eq. (30) has been applied. We note that compared to the SRT-LB model based four-level finite-difference scheme for one-dimensional equation [17], the present MRT-LB model based macroscopic numerical scheme can be more accurate through adjusting the weight coefficient  $\omega_0$  and relaxation parameters  $s_1$  and  $s_2$  to satisfy Eq. (31). In the following, some remarks on the MRT-LB model based macroscopic numerical scheme are listed.

*Remark I:* It is found that the relaxation parameter  $s_0$  corresponding to the zeroth moment of distribution function  $f_i(x, t)$  (or conservative variable  $\phi$ ) does not appear in the macroscopic numerical scheme Eq. (22), and thus it has no influence on the numerical results. This also explains why the relaxation parameter  $s_0$  in the MRT-LB method can be chosen arbitrarily. However, unlike the relaxation parameter  $s_0$ , the relaxation parameter  $s_2$  corresponding to the second-order moment of distribution function has an important influence on the macroscopic numerical scheme Eq. (22) [see Eq. (31)], and also the numerical results. Actually, these results have also been reported in some previous works on the MRT-LB model for (convection) diffusion equations [28,46,67].

*Remark II:* When the conditions of Eqs. (30) and (31) are satisfied, the MRT-LB model based macroscopic four-level numerical scheme Eq. (22) has a sixth-order accuracy in space. However, if only Eqs. (30) and (31a) hold, the macroscopic four-level numerical scheme would have a fourth-order accuracy in space. Compared to the SRT-LB model based macroscopic four-level fourth-order numerical scheme [17], the present macroscopic numerical scheme has another distinct characteristic, i.e., there is a free relaxation parameter  $s_2$ , which can be used to remove the discrete effect of anti-bounce-back scheme for the Dirichlet boundary conditions [46,67].

*Remark III:* Compared to the classical two-level LB method, the implementation of the macroscopic four-level numerical scheme needs the initial values of variable  $\phi$  at first three time levels, and usually to complete the initialization, we must adopt some other numerical schemes to obtain the values of variable  $\phi$  at the second and third time levels. In addition, the inclusion of the extra time levels also brings a larger memory requirement to store the variable  $\phi$ .

Finally, to implement the MRT-LB model based macroscopic sixth-order numerical scheme Eq. (22), we must



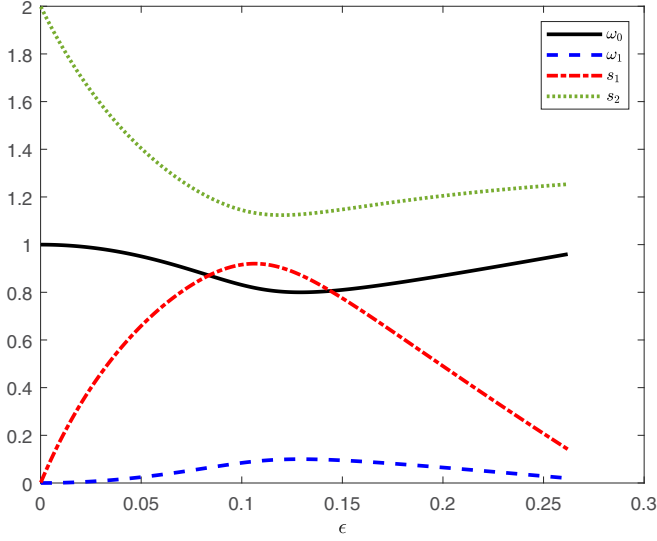


FIG. 1. The weight coefficient  $\omega_0$  and the relaxation parameters  $s_1$  and  $s_2$  as a function of the discretization parameter  $\epsilon$ .

determine the weight coefficient  $\omega_0$  and relaxation parameters  $s_1$  and  $s_2$  from Eqs. (30) and (31) for a specified  $\epsilon$ , while due to the coupling and nonlinearity of these equations, it is difficult

to derive the explicit expressions of  $\omega_0$ ,  $s_1$ , and  $s_2$  in terms of  $\epsilon$ . For this reason, we numerically solved Eqs. (30) and (31), and plotted  $\omega_0$ ,  $s_1$  and  $s_2$  as a function of the parameter  $\epsilon$  in Fig. 1. Here it should be noted that only under the condition of  $0 < \epsilon \leq \epsilon_{\max}$  with  $\epsilon_{\max}$  being about 0.262, we can obtain the real roots of Eqs. (30) and (31). As seen from Fig. 1, for a given  $\epsilon$ , the weight coefficient  $\omega_0$  and relaxation parameters  $s_1$  and  $s_2$  are located in the ranges of  $0.8 \leq \omega_0 < 1$ ,  $0 < s_1 \leq s_{1,\max}$  and  $s_{2,\min} \leq s_2 < 2.0$  with  $s_{1,\max}$  and  $s_{2,\min}$  being very close to 0.920 and 1.124.

#### IV. THE STABILITY ANALYSIS OF THE MRT-LB MODEL BASED MACROSCOPIC NUMERICAL SCHEME

In this section, we will prove that the MRT-LB model based four-level finite-difference scheme Eq. (22) is unconditionally stable. To this end, we first neglected the source term  $R$  and replaced the  $\phi_j^n$  in Eq. (10) by the distribution function  $f_{i,j}^n$  through the relation Eq. (8), and then take the discrete Fourier transform of  $f_{i,j}^n$  in Eq. (10) to obtain the following matrix equation [73],

$$\widehat{\mathbf{U}}_j^{n+1} = \mathbf{G}(\theta, \omega_0, s_1, s_2) \widehat{\mathbf{U}}_j^n, \quad (32)$$

where  $\widehat{\mathbf{U}}_j^n$  is the discrete Fourier transform of  $f_{i,j}^n$  ( $i = -1, 0, 1$ ).  $\mathbf{G}$  is the amplification matrix of the scheme, and is given by

$$\mathbf{G} = \begin{pmatrix} (1 - \frac{s_1}{2} - \frac{\omega_0 s_2}{2})e^{i\theta} & (\frac{s_2}{2} - \frac{\omega_0 s_2}{2})e^{i\theta} & (\frac{s_1}{2} - \frac{\omega_0 s_2}{2})e^{i\theta} \\ \omega_0 s_2 & \omega_0 s_2 - s_2 + 1 & \omega_0 s_2 \\ (\frac{s_1}{2} - \frac{\omega_0 s_2}{2})e^{-i\theta} & (\frac{s_2}{2} - \frac{\omega_0 s_2}{2})e^{-i\theta} & (1 - \frac{s_1}{2} - \frac{\omega_0 s_2}{2})e^{-i\theta} \end{pmatrix}, \quad (33)$$

where  $-\pi \leq \theta \leq \pi$ . However, if we take the discrete Fourier transform of Eq. (22), then one can obtain the amplification matrix  $\mathbf{H}$  of the macroscopic numerical scheme,

$$\mathbf{H} = \begin{pmatrix} 2\alpha_1 \cos \theta + \alpha_2 & 2\beta_1 \cos \theta + \beta_2 & \gamma \\ 1 & 0 & 0 \\ 0 & 1 & 0 \end{pmatrix}. \quad (34)$$

Although the amplification matrix  $\mathbf{H}$  is different from  $\mathbf{G}$ , due to the equivalence between the MRT-LB model [Eq. (2) or (10)] and the macroscopic numerical scheme Eq. (22), the characteristic polynomials of them are identical, and can be expressed as

$$p(\lambda) = \lambda^3 + p_2 \lambda^2 + p_1 \lambda + p_0, \quad (35)$$

where the coefficients  $p_0$ ,  $p_1$  and  $p_2$  are given by

$$\begin{aligned} p_0 &= (s_1 - 1)(1 - s_2), \\ p_1 &= (s_1 - 1)(s_2 \omega_0 - 1) + [(s_1 - 2)(s_2 - 1) \\ &\quad + s_2 \omega_0 (1 - s_1)] \cos \theta, \\ p_2 &= s_2 - s_2 \omega_0 - 1 + (s_2 \omega_0 + s_1 - 2) \cos \theta. \end{aligned} \quad (36)$$

In the following, we would show that the roots of the characteristic polynomial  $p(\lambda)$  denoted by  $\lambda_k$  ( $k = 1, 2$ , and 3) satisfy the condition  $|\lambda_k| \leq 1$ .

With the linear fractional transformation

$$\lambda = \frac{1+z}{1-z}, \quad z \in \mathcal{C}, \quad (37)$$

the unit circle  $|\lambda| = 1$  and the field  $|\lambda| < 1$  are mapped to the imaginary axis  $[\text{Re}(z) = 0]$  and left-half plane  $[\text{Re}(z) < 0]$ , and vice versa. Here  $\mathcal{C}$  and  $\text{Re}$  denote the complex-number field and the real part of a complex number. Substituting Eq. (37) into Eq. (35), we have

$$\begin{aligned} (1-z)^3 p\left(\frac{1+z}{1-z}\right) &= (1+z)^3 + p_2(1-z)(1+z)^2 + p_1(1-z)^2(1+z) + p_0(1-z)^3 \\ &= (1-p_0+p_1-p_2)z^3 + (3+3p_0-p_1-p_2)z^2 \\ &\quad + (3-3p_0-p_1+p_2)z + (1+p_0+p_1+p_2). \end{aligned} \quad (38)$$

To ensure that the roots of characteristic polynomial  $p(\lambda)$  are located in the field  $|\lambda| < 1$ , the following conditions must be satisfied, i.e., the Routh-Hurwitz stability criterion [74–76],

$$1 - p_0 + p_1 - p_2 > 0, \tag{39a}$$

$$3 + 3p_0 - p_1 - p_2 > 0, \tag{39b}$$

$$3 - 3p_0 - p_1 + p_2 > 0, \tag{39c}$$

$$1 + p_0 + p_1 + p_2 > 0, \tag{39d}$$

$$1 - p_1 + p_0p_2 - p_0^2 > 0. \tag{39e}$$

After the sums of Eqs. (39a) and (39c), and Eqs. (39b) and (39d), we can equivalently rewrite Eq. (39) as

$$1 - p_0 + p_1 - p_2 > 0, \tag{40a}$$

$$1 - p_0 > 0, \tag{40b}$$

$$1 + p_0 > 0, \tag{40c}$$

$$1 + p_0 + p_1 + p_2 > 0, \tag{40d}$$

$$1 - p_1 + p_0p_2 - p_0^2 > 0. \tag{40e}$$

Actually, under the condition of  $\cos \theta \neq 1$ , we can first obtain

$$1 - p_0 + p_1 - p_2 = (2 - s_1)(2 - s_2)(1 + \cos \theta) + s_1s_2\omega_0(1 - \cos \theta) > 0, \tag{41a}$$

$$1 + p_0 = 1 + (s_1 - 1)(1 - s_2) > 0, \tag{41b}$$

$$1 - p_0 = 1 - (s_1 - 1)(1 - s_2) > 0, \tag{41c}$$

$$1 + p_0 + p_1 + p_2 = s_2(1 - \cos \theta)(2 - s_1)(1 - \omega_0) > 0, \tag{41d}$$

where  $0 < \omega_0 < 1$  and  $0 < s_1, s_2 < 2$  have been used.

To prove Eq. (40e), we first introduce the parameters  $A$  and  $B$ ,

$$A = s_1(1 - s_2)(2 - s_1) + \omega_0s_2(1 - s_1)(2 - s_2),$$

$$B = s_1s_2(s_1 + s_2 - s_1s_2) = s_1s_2[1 - (1 - s_1)(1 - s_2)] > 0, \tag{42}$$

and can express the part on the left-hand side of Eq. (40e) as

$$1 - p_0^2 - p_1 + p_0p_2 = [s_1(1 - s_2)(2 - s_1) + \omega_0s_2(1 - s_1)(2 - s_2)](1 - \cos \theta) + s_1s_2(s_1 + s_2 - s_1s_2) = A(1 - \cos \theta) + B. \tag{43}$$

(i) If  $0 < s_1 \leq 1$  and  $0 < s_2 \leq 1$ , then we can obtain  $A \geq 0$  and the following equation:

$$1 - p_0^2 - p_1 + p_0p_2 = A(1 - \cos \theta) + B > 0. \tag{44}$$

(ii) If  $0 < s_1 \leq 1$  and  $1 < s_2 < 2$ , then we have

$$A = s_1(1 - s_2)(2 - s_1) + \omega_0s_2(1 - s_1)(2 - s_2) \geq s_1(1 - s_2)(2 - s_1), \tag{45}$$

which can be used to derive

$$1 - p_0^2 - p_1 + p_0p_2 \geq 2s_1(1 - s_2)(2 - s_1) + B = s_1(2 - s_2)[1 + (1 - s_1)(1 - s_2)] > 0. \tag{46}$$

(iii) If  $1 < s_1 < 2$  and  $0 < s_2 \leq 1$ , then one can obtain

$$A = s_1(1 - s_2)(2 - s_1) + \omega_0s_2(1 - s_1)(2 - s_2) > s_2(1 - s_1)(2 - s_2), \tag{47}$$

then we have

$$1 - p_0^2 - p_1 + p_0p_2 > 2s_2(1 - s_1)(2 - s_2) + B = s_2(2 - s_1)[1 + (1 - s_1)(1 - s_2)] > 0. \tag{48}$$

(iv) If  $1 < s_1 < 2$  and  $1 < s_2 < 2$ , then one can derive

$$A = s_1(1 - s_2)(2 - s_1) + \omega_0s_2(1 - s_1)(2 - s_2) > s_1(1 - s_2)(2 - s_1) + s_2(1 - s_1)(2 - s_2). \tag{49}$$

With the help of above equation and let  $C = s_1(1 - s_2)(2 - s_1) + s_2(1 - s_1)(2 - s_2)$ , we can obtain

$$1 - p_0^2 - p_1 + p_0p_2 > 2A + B > 2C + B = (2 - s_1)(2 - s_2)[1 + (s_1 - 1)(1 - s_2)] > 0. \tag{50}$$

Based on above results (i)–(iv), one can find that Eq. (40e) indeed holds under the conditions of  $0 < \omega_0 < 1$  and  $0 < s_1, s_2 < 2$ . Thus, the roots of characteristic polynomial  $p(\lambda)$  are located in the field  $|\lambda| < 1$  under the condition of  $\cos \theta \neq 1$ .



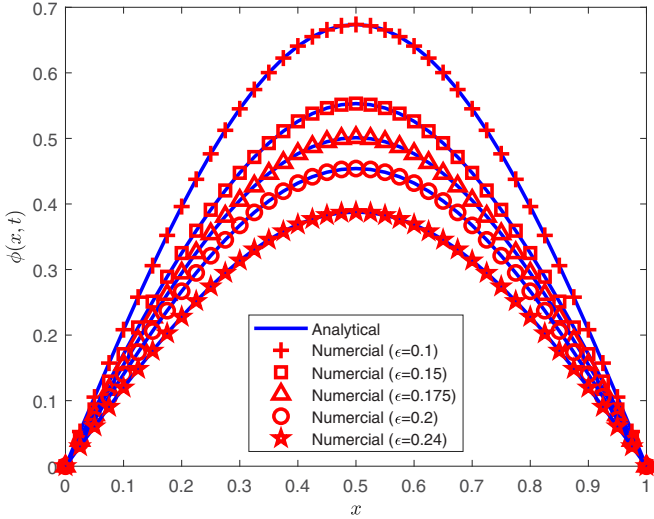


FIG. 2. The numerical and analytical solutions under different values of discretization parameter  $\epsilon$ .

Now let us focus on the case of  $\cos \theta = 1$ . We note that the roots of the characteristic polynomial  $p(\lambda)$  are continuous functions of  $\cos \theta$ , and hence the roots of characteristic polynomial satisfy the condition  $|\lambda_k| \leq 1$  ( $k = 1, 2$ , and  $3$ ). In addition, we would also like to point out that for the special case of  $\cos \theta = 1$ , one can adopt the reductive approach [77] to obtain  $|\lambda_k| \leq 1$  ( $k = 1, 2$ , and  $3$ ).

From above discussion, we can find that the roots of characteristic polynomial satisfy the condition  $|\lambda_k| \leq 1$  ( $k = 1, 2$  and  $3$ ), thus the present MRT-LB model based macroscopic numerical scheme Eq. (22) is unconditionally stable.

V. NUMERICAL RESULTS AND DISCUSSION

To test the capacity of the MRT-LB model based macroscopic four-level numerical scheme Eq. (22), we first considered the diffusion Eq. (1) with the following initial and

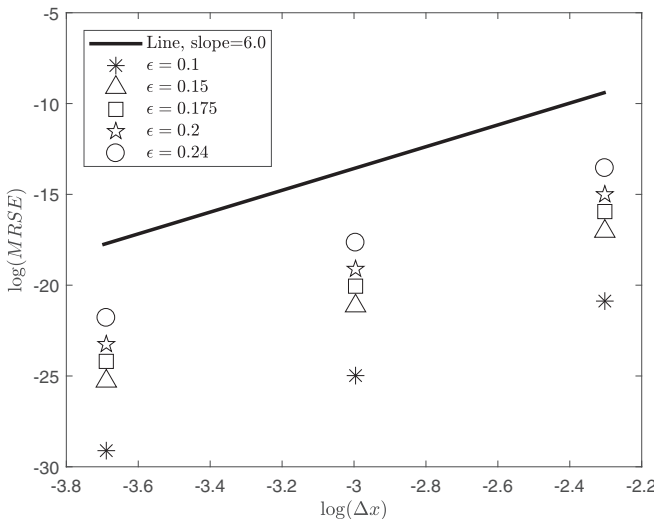


FIG. 3. The convergence rate of the MRT-LB model based macroscopic four-level finite-difference scheme under the conditions of Eqs. (30) and (31).

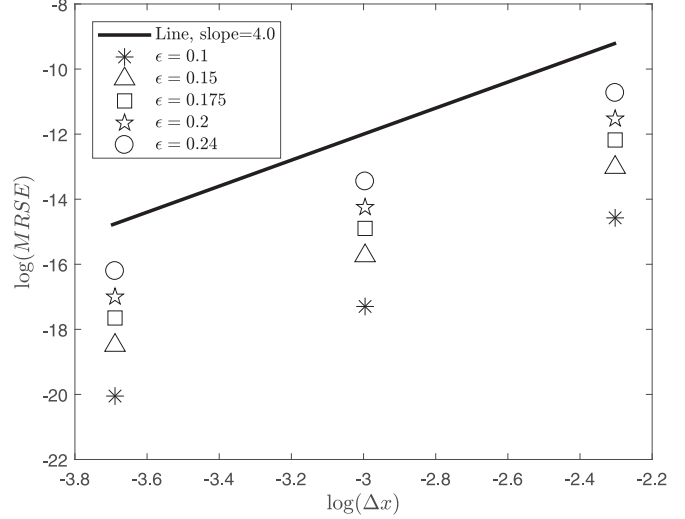


FIG. 4. The convergence rate of the MRT-LB model based macroscopic four-level finite-difference scheme under the conditions of Eqs. (30) and (31a).

boundary conditions [78],

$$\begin{aligned} \phi(x, 0) &= \sin(\pi x), \quad 0 \leq x \leq 1, \\ \phi(0, t) &= \phi(1, t) = 0, \quad t > 0, \end{aligned} \tag{51}$$

and obtained the analytical solution of this problem,

$$\phi(x, t) = \sin(\pi x)e^{-\kappa\pi^2 t}. \tag{52}$$

In the implementation of the macroscopic four-level numerical scheme Eq. (22), the analytical solution Eq. (52) is used to initialize the variable  $\phi$  at first three time levels. We first performed some simulations under different values of discretization parameter  $\epsilon$  ( $\epsilon = 0.1, 0.15, 0.175, 0.2$  and  $0.24$  corresponding to different diffusion coefficients for the specified lattice spacing  $\Delta x = 0.025$  and time step  $\Delta t = 0.01875$ ),

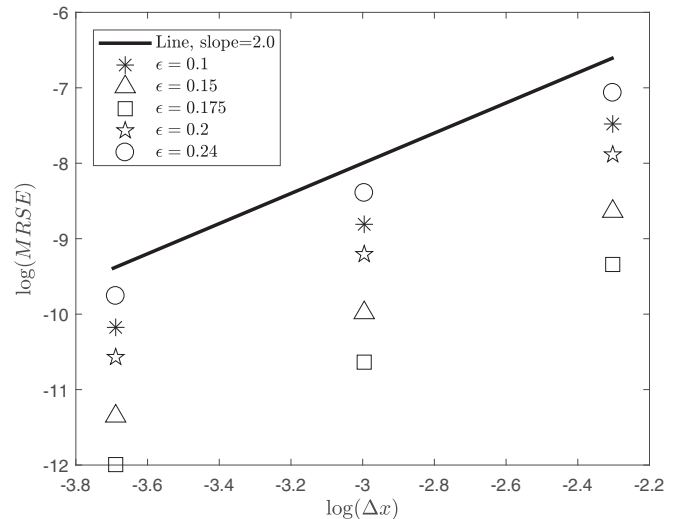


FIG. 5. The convergence rate of the MRT-LB model based macroscopic four-level finite-difference scheme under the condition of Eq. (30).

TABLE I. The values of some parameters in the MRT-LB based macroscopic four-level numerical scheme under the conditions of Eqs. (30) and (31).

$\epsilon$	$\omega_0$	$s_1$	$s_2$
0.1	0.8310204592587027	0.9159290534201945	1.1450386147380731
0.15	0.8101626131270389	0.775103705680168	1.1476236168426883
0.175	0.8370678725639358	0.6352970255557769	1.1776696173022918
0.2	0.870066309422671	0.49037716562528605	1.2047312964902426
0.24	0.9274277013170459	0.2626707812024917	1.2388413217086902

and plotted the results in Fig. 2 where the weight coefficient  $\omega_0$  and the relaxation parameters  $s_1$  and  $s_2$  are determined from Eqs. (30) and (31). As shown in this figure, the numerical results are in good agreement with the analytical solutions at time  $t = 12$ . In addition, to quantitatively measure the deviation between the numerical results and analytical solutions, the following root-mean-square error (RMSE) is adopted [17],

$$\text{RMSE} = \sqrt{\frac{\sum_{j=1}^N [\phi(j\Delta x, n\Delta t) - \phi^*(j\Delta x, n\Delta t)]^2}{N}}, \quad (53)$$

where  $N$  is the number of grid points,  $\phi$  and  $\phi^*$  are the numerical and analytical solutions. Based on the definition of RMSE, one can evaluate the convergence rate ( $C_R$ ) of numerical scheme with the following formula,

$$C_R = \log(\text{RMSE}_{\Delta x}/\text{RMSE}_{\Delta x/2})/\log 2. \quad (54)$$

We now focus on the RMSE and convergence rate of the macroscopic four-level numerical scheme Eq. (22). For this purpose, we conducted some simulations under different values of space step  $\Delta x$  and discretization parameter  $\epsilon$  [see Table I for details, the weight coefficient  $\omega_0$  and relaxation parameters  $s_1$  and  $s_2$  are given by Eqs. (30) and (31)], and measured the RMSE between the analytical and numerical solutions at time  $t = 12$ . As seen from Table II and Fig. 3, the MRT-LB model based macroscopic four-level numerical scheme indeed has a sixth-order convergence rate in space once the conditions of Eqs. (30) and (31) are satisfied, and the numerical results with a smaller discretization parameter  $\epsilon$  are more accurate. However, as demonstrated in the previous accuracy analysis, if the conditions of Eqs. (30) and (31) are not met, then the MRT-LB model based macroscopic numerical scheme could not achieve the sixth-order accuracy in space. To confirm this statement, we also carried out some simulations under the conditions of Eqs. (30) and (31a) [Eq. (31b) is not satisfied], and presented the errors at different space steps in Table III and Fig. 4. From these table and figure, one can observe that the MRT-LB model based macroscopic four-level numerical scheme is just fourth-order accurate in

space. Moreover, if both Eqs. (31a) and (31b) are not satisfied in our simulations, then the MRT-LB model based macroscopic four-level numerical scheme, as the commonly used LB method [28], only has a second-order convergence rate, as reported in Table IV and Fig. 5. We note that these results are in agreement with our theoretical analysis.

In the following, we continue to investigate another diffusion problem with the following initial condition [79],

$$\phi(x, 0) = \delta(x), \quad (55)$$

where  $\delta(x)$  is the  $\delta$  function. Under this condition, one can obtain the analytical solution of the particle probability density  $\phi$ ,

$$\phi(x, t) = \frac{1}{\sqrt{4\pi\kappa t}} e^{-\frac{x^2}{4\kappa t}}, \quad (56)$$

and its second-order moment,

$$\frac{1}{\sqrt{4\pi\kappa t}} \int_{-\infty}^{\infty} x^2 e^{-\frac{x^2}{4\kappa t}} dx = 2\kappa t. \quad (57)$$

Similar to the discussion in the previous work [79], initially if we only know the particle inside a lattice cell centered around the origin with the width  $\Delta x$ , then the density  $\phi$  can be given by

$$\phi(x, t) = \frac{1}{2\Delta x} \left[ \text{erf} \left( \frac{x + \Delta x/2}{2\sqrt{\kappa t}} \right) - \text{erf} \left( \frac{x - \Delta x/2}{2\sqrt{\kappa t}} \right) \right], \quad (58)$$

which leads to the following second-order moment,

$$\int_{-\infty}^{\infty} x^2 \phi(x, t) dx = 2\kappa t + \frac{(\Delta x)^2}{12}, \quad (59)$$

and its dimensionless form,

$$M_2 = \frac{1}{\Delta x^2} \sum_{i=-\infty}^{\infty} \int_{i\Delta x - \frac{\Delta x}{3}}^{i\Delta x + \frac{\Delta x}{3}} x^2 \phi(x, t) dx. \quad (60)$$

TABLE II. The RMSE and  $C_R$  of the MRT-LB based macroscopic four-level numerical scheme under the conditions of Eqs. (30) and (31).

$\epsilon$	$\text{RMSE}_{\Delta x=0.1}$	$\text{RMSE}_{\Delta x=0.05}$	$\text{RMSE}_{\Delta x=0.025}$	$C_R$
0.1	$8.59 \times 10^{-10}$	$1.42 \times 10^{-11}$	$2.57 \times 10^{-13}$	$\sim 5.85$
0.15	$3.99 \times 10^{-8}$	$6.56 \times 10^{-10}$	$1.04 \times 10^{-11}$	$\sim 5.95$
0.175	$1.19 \times 10^{-7}$	$1.95 \times 10^{-9}$	$3.11 \times 10^{-11}$	$\sim 5.95$
0.2	$3.04 \times 10^{-7}$	$5.00 \times 10^{-9}$	$7.96 \times 10^{-11}$	$\sim 5.95$
0.24	$1.31 \times 10^{-6}$	$2.15 \times 10^{-8}$	$3.43 \times 10^{-10}$	$\sim 5.95$

TABLE III. The RMSE and  $C_R$  of the MRT-LB based macroscopic four-level numerical scheme under the conditions of Eqs. (30) and (31a).

$\epsilon$	$\omega_0$	$s_1$	$s_2$	RMSE $_{\Delta x=0.1}$	RMSE $_{\Delta x=0.05}$	RMSE $_{\Delta x=0.025}$	$C_R$
0.1	0.8	1	12/11	$4.68 \times 10^{-7}$	$3.08 \times 10^{-8}$	$1.96 \times 10^{-9}$	$\sim 3.95$
0.15	0.7	1	42/41	$2.21 \times 10^{-6}$	$1.46 \times 10^{-7}$	$9.30 \times 10^{-9}$	$\sim 3.95$
0.175	0.65	1	78/79	$5.13 \times 10^{-6}$	$3.39 \times 10^{-7}$	$2.16 \times 10^{-8}$	$\sim 3.95$
0.2	0.6	1	18/19	$9.84 \times 10^{-6}$	$6.49 \times 10^{-7}$	$4.14 \times 10^{-8}$	$\sim 3.95$
0.24	0.52	1	78/89	$2.19 \times 10^{-5}$	$1.44 \times 10^{-6}$	$9.16 \times 10^{-8}$	$\sim 3.95$

In our simulations, the discrete second-order moment corresponding to Eq. (60) is computed by

$$m_2 = \sum_{i=-\infty}^{\infty} i^2 \phi(i\Delta x, t) \Delta x. \quad (61)$$

We carried our some numerical experiments with the computational domain  $[-10, 10]$ , and conducted a comparison between the theoretical and numerical results of second-order moment in Fig. 6, where  $t = 12$ ,  $\kappa = 1.5 \times 10^{-4}$ ,  $\epsilon = 0.15$ ,  $\omega_0 = 0.813013333656164$ ,  $s_1 = 0.918883500649446$ , and  $s_2 = 1.128626937193323$  (see Table I). To ensure that  $N = t/\Delta t$  is an integer, the time steps in our simulations are set as  $\Delta t = 0.6, 0.8, 1.0, 1.2, 1.5, 2.0, 2.4, 3.0, 4.0, 6.0, 12.0$ , which would result in different values of lattice spacing  $\Delta x$  according to Eq. (30). As seen from this figure, the calculated discrete second-order moment ( $m_2$ ) converges to  $a^2 + 0.08347$ , which is very close to the theoretical value  $a^2 + 1/12$  with  $a^2 = 2\kappa t/(\Delta x)^2$  [79].

In addition, if we substitute Eq. (61) into Eq. (59), then one can obtain

$$a^2 = m_2 - \frac{1}{12}. \quad (62)$$

However, according to Eq. (30), we can derive the relation between  $a^2$  and  $\omega_0$ ,

$$a^2 = 2(1 - \omega_0) \left( \frac{1}{s_1} - \frac{1}{2} \right) \frac{t}{\Delta t}. \quad (63)$$

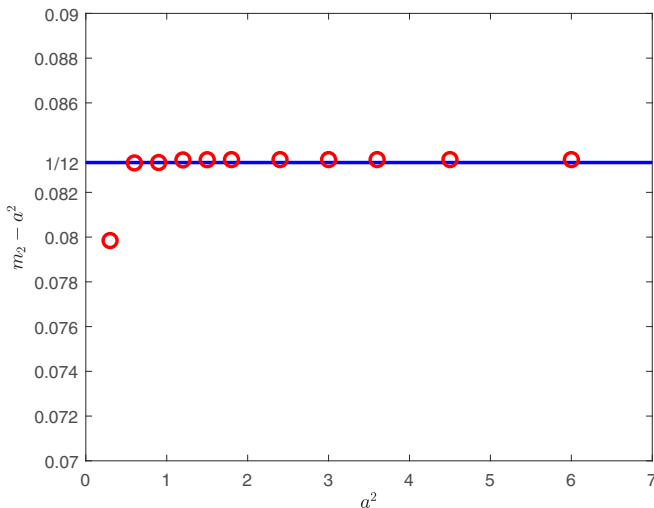


FIG. 6. A comparison between the theoretical (solid line) and numerical (symbols) results of second-order moment.

From Fig. 7 where  $\Delta t = 0.2$  and  $t = 12$ , one can find that the numerical results are in good agreement with the theoretical solution of  $a^2$  [Eq. (63)] in the range of  $0.8 \leq \omega_0 < 1$ .

### VI. CONCLUSIONS

In this work, we first developed a MRT-LB model for one-dimensional diffusion equation where the D1Q3 lattice structure is considered, and then obtained a mesoscopic MRT-LB model based macroscopic four-level finite-difference scheme. Through the theoretical analysis, one can find that the macroscopic four-level numerical scheme is unconditionally stable, and can achieve the sixth-order accuracy in space once the weight coefficient  $\omega_0$  and the relaxation parameters  $s_1$  and  $s_2$  satisfy Eqs. (30) and (31). And also, if only the conditions of Eqs. (30) and (31a) are met, then the macroscopic four-level numerical scheme would have a fourth-order convergence rate in space. Moreover, if only Eq. (30) is satisfied, then the macroscopic four-level numerical scheme would be second-order accurate in space, which is the same as the commonly used LB method. In addition, compared to the previous work [17], the present macroscopic numerical scheme could be more accurate through adjusting the weight coefficient  $\omega_0$  and the relaxation parameters  $s_1$  and  $s_2$  properly.

We also conducted some simulations to test the MRT-LB model based macroscopic four-level finite-difference scheme,

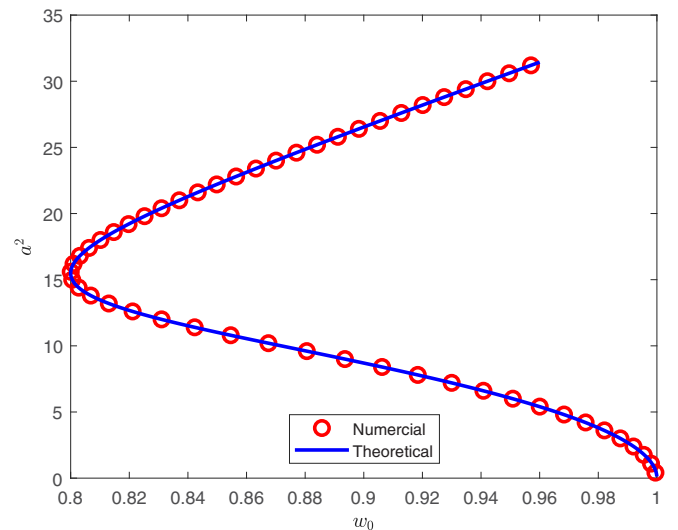


FIG. 7. A comparison between the numerical and theoretical results of  $a^2$ .

TABLE IV. The RMSE and  $C_R$  of the MRT-LB based macroscopic four-level numerical scheme under the condition of Eq. (30) [Eqs. (31a) and (31b) are not satisfied].

$\epsilon$	$\omega_0$	$s_1$	$s_2$	RMSE $_{\Delta x=0.1}$	RMSE $_{\Delta x=0.05}$	RMSE $_{\Delta x=0.025}$	$C_R$
0.1	0.8	1	1	$5.65 \times 10^{-4}$	$1.49 \times 10^{-4}$	$3.81 \times 10^{-5}$	$\sim 1.95$
0.15	0.7	1	1	$1.77 \times 10^{-4}$	$4.62 \times 10^{-5}$	$1.17 \times 10^{-5}$	$\sim 1.96$
0.175	0.65	1	1	$8.77 \times 10^{-5}$	$2.40 \times 10^{-5}$	$6.18 \times 10^{-6}$	$\sim 1.91$
0.2	0.6	1	1	$3.76 \times 10^{-4}$	$1.00 \times 10^{-4}$	$2.57 \times 10^{-5}$	$\sim 1.93$
0.24	0.52	1	1	$8.55 \times 10^{-4}$	$2.27 \times 10^{-4}$	$5.79 \times 10^{-5}$	$\sim 1.94$

and found that the numerical results agree well our theoretical analysis.

Finally, we would like to point out that in the D1Q3 LB method based macroscopic numerical schemes, the present macroscopic numerical scheme Eq. (22) with the sixth-order convergence rate is the most accurate for one-dimensional diffusion equations. We also note that the present results are only limited to one-dimensional case, the MRT-LB model based macroscopic numerical schemes for two and three-

dimensional diffusion problems would be considered in a future work.

### ACKNOWLEDGMENTS

This work was financially supported by the National Natural Science Foundation of China (Grants No. 12072127 and No. 51836003) and the National Key Research and Development Program of China (Grant No. 2017YFE0100100).

- [1] R. Benzi, S. Succi, and M. Vergassola, The lattice Boltzmann equation: Theory and applications, *Phys. Rep.* **222**, 145 (1992).
- [2] S. Chen and G. Doolen, Lattice Boltzmann method for fluid flows, *Annu. Rev. Fluid Mech.* **30**, 329 (1998).
- [3] C. K. Aidun and J. R. Clausen, Lattice-Boltzmann method for complex flows, *Annu. Rev. Fluid Mech.* **42**, 439 (2010).
- [4] L. Chen, Q. Kang, Y. Mu, Y.-L. He, and W.-Q. Tao, A critical review of the pseudopotential multiphase lattice Boltzmann model: Methods and applications, *Int. J. Heat Mass Transf.* **76**, 210 (2014).
- [5] Q. Li, K. H. Luo, Q. J. Kang, Y. L. He, Q. Chen, and Q. Liu, Lattice Boltzmann methods for multiphase flow and phase-change heat transfer, *Prog. Energy Combust. Sci.* **52**, 62 (2016).
- [6] H. Liu, Q. Kang, C. R. Leonardi, S. Schmieschek, A. Narváez, B. D. Jones, J. R. Williams, A. J. Valocchi, and J. Harting, Multiphase lattice Boltzmann simulations for porous media applications, *Comput. Geosci.* **20**, 777 (2016).
- [7] H. Wang, X. Yuan, H. Liang, Z. Chai, and B. Shi, A brief review of the phase-field-based lattice Boltzmann method for multiphase flows, *Capillary* **2**, 33 (2019).
- [8] K. V. Sharma, R. Straka, and F. W. Tavares, Current status of lattice Boltzmann methods applied to aerodynamic, aeroacoustic, and thermal flows, *Prog. Aero. Sci.* **115**, 100616 (2020).
- [9] D. A. Wolf-Gladrow, *Lattice-Gas Cellular Automata and Lattice Boltzmann Models: An Introduction* (Springer, Berlin, 2000).
- [10] S. Succi, *The Lattice Boltzmann Equation for Fluid Dynamics and Beyond* (Oxford University Press, Oxford, 2001).
- [11] M. C. Sukop and D. T. Thorne, Jr., *Lattice Boltzmann Modeling: An Introduction for Geoscientists and Engineers* (Springer, New York, 2006).
- [12] Z. Guo and C. Shu, *Lattice Boltzmann Method and Its Applications in Engineering* (World Scientific Publishing, Singapore, 2013).
- [13] T. Krüger, H. Kusumaatmaja, A. Kuzmin, O. Shardt, G. Silva, and E. M. Viggien, *The Lattice Boltzmann Method: Principles and Practice* (Springer, Switzerland, 2017).
- [14] S. P. Dawson, S. Chen, and G. D. Doolen, Lattice Boltzmann computations for reaction-diffusion equations, *J. Chem. Phys.* **98**, 1514 (1993).
- [15] D. A. Wolf-Gladrow, A lattice Boltzmann equation for diffusion, *J. Stat. Phys.* **79**, 1023 (1995).
- [16] C. Huber, B. Chopard, and M. Manga, A lattice Boltzmann model for coupled diffusion, *J. Comput. Phys.* **229**, 7956 (2010).
- [17] S. Suga, An accurate multi-level finite difference scheme for 1D diffusion equations derived from the lattice Boltzmann method, *J. Stat. Phys.* **140**, 494 (2010).
- [18] P. V. Leemput, C. Vandekerckhove, W. Vanroose, and D. Roose, Accuracy of hybrid lattice Boltzmann/finite difference schemes for reaction-diffusion systems, *Multiscale Model. Simul.* **6**, 838 (2007).
- [19] R. G. M. van der Sman and M. H. Ernst, Convection-diffusion lattice Boltzmann scheme for irregular lattices, *J. Comput. Phys.* **160**, 766 (2000).
- [20] I. Ginzburg, Equilibrium-type and link-type lattice Boltzmann models for generic advection and anisotropic-dispersion equation, *Adv. Water Resour.* **28**, 1171 (2005).
- [21] I. Rasin, S. Succi, and W. Miller, A multi-relaxation lattice kinetic method for passive scalar diffusion, *J. Comput. Phys.* **206**, 453 (2005).
- [22] I. Ginzburg, Multiple anisotropic collisions for advection-diffusion lattice Boltzmann schemes, *Adv. Water Resour.* **51**, 381 (2013).
- [23] B. Shi and Z. Guo, Lattice Boltzmann model for nonlinear convection-diffusion equations, *Phys. Rev. E* **79**, 016701 (2009).
- [24] B. Chopard, J. L. Falcone, and J. Latt, The lattice Boltzmann advection-diffusion model revisited, *Eur. Phys. J. Spec. Top.* **171**, 245 (2009).
- [25] H. Yoshida and M. Nagaoka, Multiple-relaxation-time lattice Boltzmann model for the convection and anisotropic diffusion equation, *J. Comput. Phys.* **229**, 7774 (2010).
- [26] Z. Chai and T. S. Zhao, Lattice Boltzmann model for the convection-diffusion equation, *Phys. Rev. E* **87**, 063309 (2013).

- [27] R. Huang and H. Wu, A modified multiple-relaxation-time lattice Boltzmann model for convection-diffusion equation, *J. Comput. Phys.* **274**, 50 (2014).
- [28] Z. Chai, B. Shi, and Z. Guo, A multiple-relaxation-time lattice Boltzmann model for general nonlinear anisotropic convection-diffusion equations, *J. Sci. Comput.* **69**, 355 (2016).
- [29] O. Aursjø, E. Jettestuen, J. L. Vinningland, and A. Hiorth, An improved lattice Boltzmann method for simulating advective-diffusive processes in fluids, *J. Comput. Phys.* **332**, 363 (2017).
- [30] L. Li, Multiple-time-scaling lattice Boltzmann method for the convection diffusion equation, *Phys. Rev. E* **99**, 063301 (2019).
- [31] M. Hirabayashi, Y. Chen, and H. Ohashi, The lattice BGK model for the Poisson equation, *JSME Int. J. Ser. B* **44**, 45 (2001).
- [32] Z. Chai and B. Shi, A novel lattice Boltzmann model for the Poisson equation, *Appl. Math. Model.* **32**, 2050 (2008).
- [33] Z. Chai, H. Liang, R. Du, and B. Shi, A lattice Boltzmann model for two-phase flow in porous media, *SIAM J. Sci. Comput.* **41**, B746 (2019).
- [34] H. Lai and C. Ma, Lattice Boltzmann method for the generalized Kuramoto-Sivashinsky equation, *Physica A* **388**, 1405 (2009).
- [35] H. Otomo, B. M. Boghosian, and F. Dubois, Two complementary lattice-Boltzmann-based analyses for nonlinear systems, *Physica A* **486**, 1000 (2017).
- [36] Z. Chai, N. He, Z. Guo, and B. Shi, Lattice Boltzmann model for high-order nonlinear partial differential equations, *Phys. Rev. E* **97**, 013304 (2018).
- [37] L. Zhong, S. Feng, P. Dong, and S. Gao, Lattice Boltzmann schemes for the nonlinear Schrödinger equation, *Phys. Rev. E* **74**, 036704 (2006).
- [38] S. Succi, Lattice Boltzmann method for quantum field theory, *J. Phys. A* **40**, F559 (2007).
- [39] S. Palpacelli and S. Succi, Numerical validation of the quantum lattice Boltzmann scheme in two and three dimensions, *Phys. Rev. E* **75**, 066704 (2007).
- [40] B. Shi and Z. Guo, Lattice Boltzmann model for the one-dimensional nonlinear Dirac equation, *Phys. Rev. E* **79**, 066704 (2009).
- [41] Y. H. Qian, D. d’Humières, and P. Lallemand, Lattice BGK models for Navier-Stokes equation, *Europhys. Lett.* **17**, 479 (1992).
- [42] D. d’Humières, Generalized lattice-Boltzmann equations, in *Rarefied Gas Dynamics: Theory and Simulations*, in Prog. Astronaut. Aeronaut., Vol. 159, edited by B. D. Shizgal and D. P. Weave (AIAA, Washington, DC, 1992), pp. 450–458.
- [43] Z. Chai and B. Shi, Multiple-relaxation-time lattice Boltzmann method for the Navier-Stokes and nonlinear convection-diffusion equations: Modeling, analysis, and elements, *Phys. Rev. E* **102**, 023306 (2020).
- [44] P. Lallemand and L.-S. Luo, Theory of the lattice Boltzmann method: Dispersion, dissipation, isotropy, Galilean invariance, and stability, *Phys. Rev. E* **61**, 6546 (2000).
- [45] C. Pan, L.-S. Luo, C. T. Miller, An evaluation of lattice Boltzmann schemes for porous medium flow simulation, *Comput. Fluids* **35**, 898 (2006).
- [46] S. Cui, N. Hong, B. Shi, and Z. Chai, Discrete effect on the halfway bounce-back boundary condition of multiple-relaxation-time lattice Boltzmann model for convection-diffusion equations, *Phys. Rev. E* **93**, 043311 (2016).
- [47] L.-S. Luo, W. Liao, X. Chen, Y. Peng, and W. Zhang, Numerics of the lattice Boltzmann method: Effects of collision models on the lattice Boltzmann simulations, *Phys. Rev. E* **83**, 056710 (2011).
- [48] S. Chapman and T. G. Cowling, *The Mathematical Theory of Nonuniform Gases* (Cambridge University Press, Cambridge, 1970).
- [49] E. Ikenberry and C. Truesdell, On the pressures and the flux of energy in a gas according to Maxwell’s kinetic theory, I, *J. Ration. Mech. Anal.* **5**, 1 (1956).
- [50] W.-A. Yong, W. Zhao, and L.-S. Luo, Theory of the lattice Boltzmann method: Derivation of macroscopic equations via the Maxwell iteration, *Phys. Rev. E* **93**, 033310 (2016).
- [51] D. J. Holdych, D. R. Noble, J. G. Georgiadis, and R. O. Buckius, Truncation error analysis of lattice Boltzmann methods, *J. Comput. Phys.* **193**, 595 (2004).
- [52] A. Wagner, Thermodynamic consistency of liquid-gas lattice Boltzmann simulations, *Phys. Rev. E* **74**, 056703 (2006).
- [53] F. Dubois, Equivalent partial differential equations of a lattice Boltzmann scheme, *Comput. Math. Appl.* **55**, 1441 (2008).
- [54] D. d’Humières and I. Ginzburg, Viscosity independent numerical errors for lattice Boltzmann models: From recurrence equations to “magic” collision numbers, *Comput. Math. Appl.* **58**, 823 (2009).
- [55] I. Ginzburg, Truncation errors, exact and heuristic stability analysis of two-relaxation-times lattice Boltzmann schemes for anisotropic advection-diffusion equation, *Commun. Comput. Phys.* **11**, 1439 (2012).
- [56] M. Junk, A. Klar, and L.-S. Luo, Asymptotic analysis of the lattice Boltzmann equation, *J. Comput. Phys.* **210**, 676 (2005).
- [57] F. Dubois, Third order equivalent equation of lattice Boltzmann scheme, *Discret. Contin. Dyn. Syst.* **23**, 221 (2009).
- [58] F. Dubois and P. Lallemand, Towards higher order lattice Boltzmann schemes, *J. Stat. Mech.* (2009) P06006.
- [59] M. Junk, A finite difference interpretation of the lattice Boltzmann method, *Numer. Meth. Part. Diff. Equ.* **17**, 383 (2001).
- [60] T. Inamuro, A lattice kinetic scheme for incompressible viscous flows with heat transfer, *Philos. Trans. R. Soc. Lond. A* **360**, 477 (2002).
- [61] M. G. Ancona, Fully-Lagrangian and lattice-Boltzmann methods for solving systems of conservation equations, *J. Comput. Phys.* **115**, 107 (1994).
- [62] E. C. Du Fort, and S. P. Frankel, Stability conditions in the numerical treatment of parabolic differential equations, *Math. Comput.* **7**, 135 (1953).
- [63] X. He, Q. Zou, L.-S. Luo, and M. Dembo, Analytic solutions of simple flows and analysis of nonslip boundary conditions for the lattice Boltzmann BGK model, *J. Stat. Phys.* **87**, 115 (1997).
- [64] Z. Guo and C. Zheng, Analysis of lattice Boltzmann equation for microscale gas flows: Relaxation times, boundary conditions and the Knudsen layer, *Int. J. Comput. Fluid Dyn.* **22**, 465 (2008).
- [65] Z. Chai, B. Shi, Z. Guo, and J. Lu, Gas flow through square array of circular cylinders with Klinkenberg effect: A lattice Boltzmann study, *Commun. Comput. Phys.* **8**, 1052 (2010).
- [66] Q. Li, Z. Zheng, S. Wang, and J. Liu, A multilevel finite difference scheme for one-dimensional Burgers equation derived from the lattice Boltzmann method, *J. Appl. Math.* **2012**, 925920 (2012).

- [67] Z. Chai, C. Huang, B. Shi, and Z. Guo, A comparative study on the lattice Boltzmann models for predicting effective diffusivity of porous media, *Int. J. Heat Mass Transf.* **98**, 687 (2016).
- [68] J. Latt and B. Chopard, Lattice Boltzmann method with regularized pre-collision distribution functions, *Math. Comput. Simul.* **72**, 165 (2016).
- [69] L. Wang, B. Shi, and Z. Chai, Regularized lattice Boltzmann model for a class of convection-diffusion equations, *Phys. Rev. E* **92**, 043311 (2015).
- [70] X. Yang, B. Shi, and Z. Chai, Generalized modification in the lattice Bhatnagar-Gross-Krook model for incompressible Navier-Stokes equations and convection-diffusion equations, *Phys. Rev. E* **90**, 013309 (2014).
- [71] L. Wang, J. Mi, X. Meng, and Z. Guo, A localized mass-conserving lattice Boltzmann approach for non-Newtonian fluid flows, *Commun. Comput. Phys.* **17**, 908 (2015).
- [72] L. Wang, W. Zhao, and X.-D. Wang, Lattice kinetic scheme for the Navier-Stokes equations coupled with convection-diffusion equations, *Phys. Rev. E* **98**, 033308 (2018).
- [73] J. W. Thomas, *Numerical Partial Differential Equations: Finite Difference Methods* (Springer, New York, 1995).
- [74] E. J. Routh, *A Treatise of the Stability of a Given State of Motion* (Macmillan, London, 1877).
- [75] A. Hurwitz, Ueber die Bedingungen, unter welchen eine Gleichung nur Wurzeln mit negativen reellen Theilen besitzt, *Math. Ann.* **46**, 273 (1895).
- [76] F. R. Gantmacher, *Applications of the Theory of Matrices* (Interscience Publishers, New York, 1959).
- [77] J. H. Miller, On the location of zeros of certain classes of polynomials with applications to numerical analysis, *J. Inst. Maths Applics* **8**, 397 (1971).
- [78] C. A. J. Fletcher, *Computational Techniques for Fluid Dynamics 1: Fundamental and General Techniques*, 2nd ed. (Springer, Berlin, 1991).
- [79] M. R. Parsa and A. J. Wagner, Lattice gas with molecular dynamics collision operator, *Phys. Rev. E* **96**, 013314 (2017).